STUDIES OF HALO DISTRIBUTIONS UNDER BEAM-BEAM INTERACTION†

T. Chen, J. Irwin, R. H. Siemann, Stanford Linear Accelerator Center, Stanford University, Stanford, CA 94309 USA

The halo distribution due to the beam-beam interaction in circular electron-positron colliders is simulated with a program which uses a technique that saves a factor of hundreds to thousands of CPU time [1,2]. The distribution and the interference between the beam-beam interaction and lattice nonlinearities has been investigated. The effects on the halo distribution due to radiation damping, misalignment at the collision point, and chromatic effect are presented.

I. INTRODUCTION

The leap-frog simulation method[1] makes the study of the beam-beam halo distribution much more efficient, provides the ability to look into many problems that were difficult or impossible. Using a simulation code, we have studied various beam-beam effects for two existing colliders and for PEP-II B-factory design. In this paper, we present the results of these efforts.

II. THE LATTICE NONLINEARITIES—TUNE SHIFT WITH AMPLITUDES

In previous studies, we have shown that resonances are the dominant effect in tail formation[2], as evidenced by the fact that the distributions follow resonances locations. The locations of resonances are not only determined by the beam-beam kick potential, but also by the nonlinearities of the lattice, primarily the tune shifts with amplitudes.

Figure 1(a) shows the tail distribution of PEP-II HER from the beam-beam interaction. The lattice is linear and the parameters can be found in [3]. The beam distribution contour lines are steps of the logarithm of numbers in transverse amplitude space. The symbols plotted over the distribution contour lines are the locations of resonances. The few selected resonances believed to be relevant are plotted. The locations of the resonances are calculated by first order perturbation theory using beam-beam potential.

When lattice nonlinearities are added, the tune shifts with amplitudes from the beam-beam interaction and the lattice nonlinearities must be combined. As a result, resonance lines move. It is easy to imagine that the tail distribution will follow the move, and this has been observed in most of our simulations.

However, the lattice tune shift can do more than change the ridge locations at large amplitudes, and the change of the tail distribution can be dramatic. The change at medium amplitudes is important also. One example of PEP-II HER is shown in figure 1. In figure 1(b), the lattice tune shifts are included. At large vertical amplitude, resonances $2Q_x+6Q_y=5$ and $6Q_y+3Q_s=4$ are at almost the same location. The tune shift terms dQ_x/dA_x^2 and dQ_y/dA_y^2 are small, but the larger crossing terms $dQ_x/dA_y^2=dQ_y/dA_x^2$ are large. They move the two resonances close to the core where there are many more particles that now stream to large amplitudes. This produces the dramatic change in the distribution, that we see in figure 1(b).

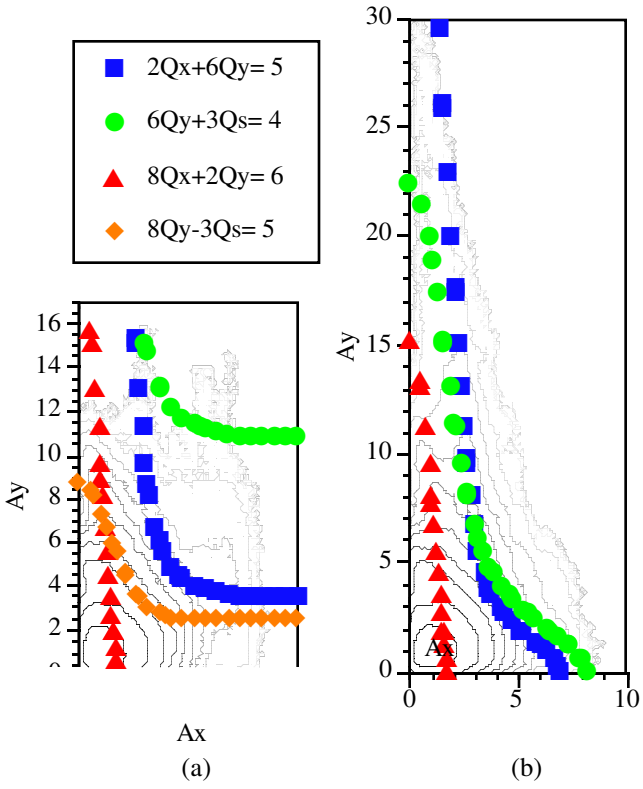

Figure 1: The beam tail distributions of PEP-II HER (a) with linear lattice, and (b) with nonlinear tune shift with amplitudes: $dQ_x/dA_x^2=-85.6$, $dQ_x/dA_y^2=dQ_y/dA_x^2=-3931$, $dQ_y/dA_y^2=-2.1$.

III. ACTION OF MULTIPLE RESONANCES

The resonance streaming and phase convection theory [4,5] have predicted the role of resonances in forming the tail and are verified by our simulation. In addition, we found that in many cases the same particle may be trapped

† Work supported by Department of Energy contracts DE-AC03-76SF00515 and DE-AC05-84ER40150

in a few resonances simultaneously, rather than streaming in a single resonance. This is shown in an investigation for the PEP-II HER with a linear lattice, the case in figure 1(a).

Study concentrates on the ridge in the distribution at about 1 σ_x and extending from 8 to 12 σ_y. A single particle was launched at 1 σ_x and 9 σ_y, and tracked for 1000 turns. The location of the particle in amplitude space turn by turn is plotted in figure 2. One can see this particle is roaming around the ridge, and presumably it is a typical particle contributing to it. The particle's phases are found on every turn. They are plotted in Φ_y versus Φ_x and Φ_s versus Φ_y in figure 2. The phase relationship indicates the particle is trapped in the $4Q_x+Q_y$ resonance most of the time, and $8Q_y-3Q_s$ all the time. Due to the symmetry of the beam-beam force, there should be no odd order transverse resonances. So, we believe the resonance $4Q_x+Q_y$ should be $8Q_x+2Q_y$. Both resonances are plotted in the distribution plot. One can see the particle has been moving between them.

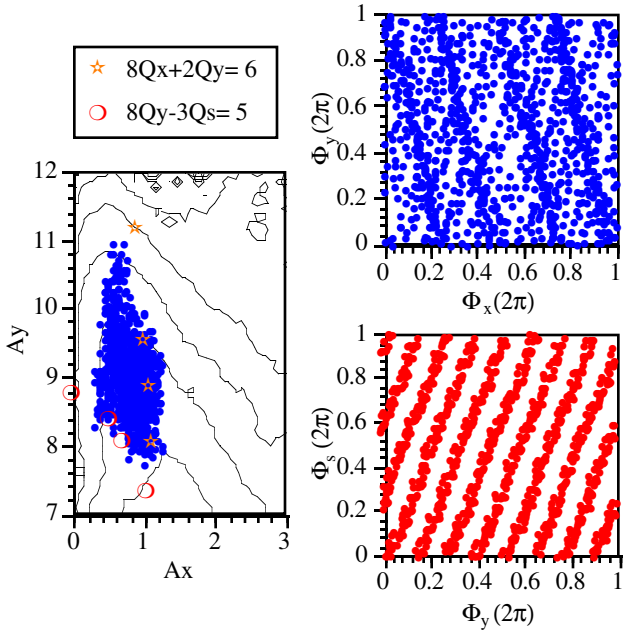

Figure 2: A particle trapped in two resonances. Plots show the particle motion in amplitude and phases.

It is also interesting to see a particle switch between resonances and change behavior. Take the case of figure 1(b), and launch a test particle at A_x=2.5 σ_x and A_y=13.5 σ_y to study the large tail. We found in the first 260 turns, the particle dropped from 13.5 σ_y to 8.5 σ_y. Then, the particle climbed up to 12 σ_y in the next 250 turns. The phases of the particle is plotted in figure 3. A cross is used for the time when the vertical amplitude was falling and a circle for when it was increasing. One can see the particle certainly has different resonance features. In addition, multiple resonances acting together may form an "island" structure in phase plot, as shown in the Φ_s versus Φ_y plot for the falling period.

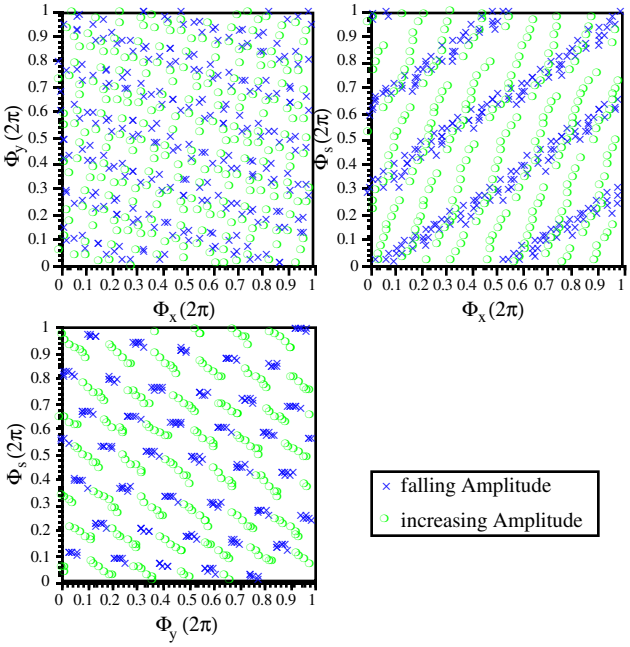

Figure 3. Phase plots of a particle during the period of falling and increasing amplitude. Different resonances are shown for each period.

IV. THE EFFECT OF SYNCHROTRON RADIATION

We know that the synchrotron radiation plays an important role in the tail distribution. It may damp the amplitude of a particle, but it may also help resonance streaming. With our program, the effect of radiation on the beam halo is simulated for the first time. Generally

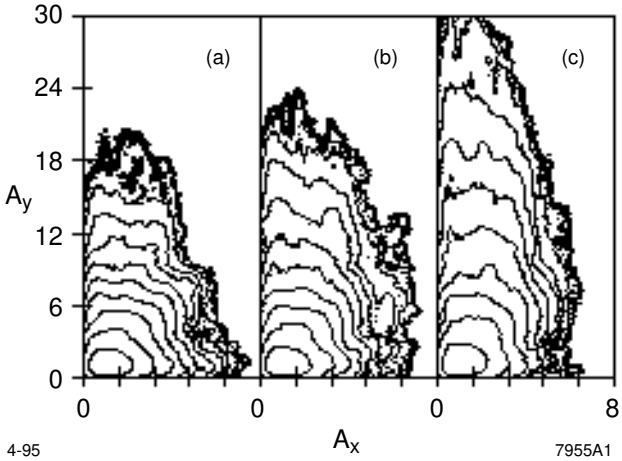

Figure 4. Beam-beam tail distributions with different radiation damping: (a) 5,000 turns; (b) 10,000 turns; (c) 20,000 turns.

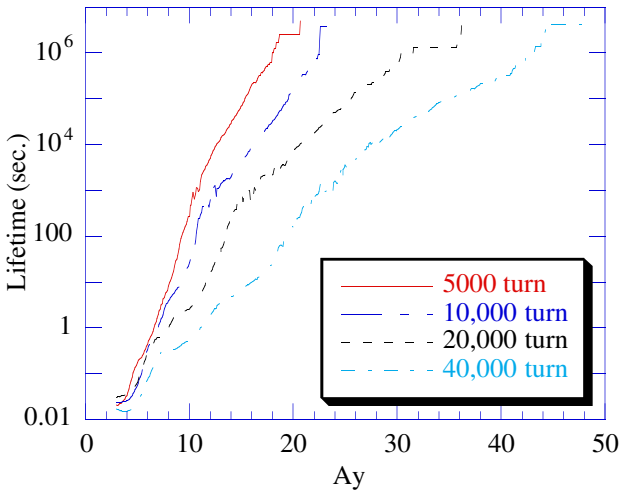

Figure 5. Lifetime as a function of vertical aperture with different radiation damping times (5000-40,000 turns).

speaking, the stronger the radiation, the shorter the vertical tail. The radiation damping seems to have little effect in the horizontal tail.

We studied the radiation effect of PEP-II LER. The parameters used are the same as CDR [3] except the tunes were Q_x=0.63, Q_y=0.552, Q_s=0.2477, and momentum compaction factor was α=0.00131. In figure 4, the tail distributions are plotted for different radiation damping times. Figure 4(a) has the design damping time of 5000 turns. With less radiation damping, the vertical tail extends farther. The lifetime as a function of vertical aperture is shown in figure 5.

V. EFFECT OF MISALIGNMENT AT IP

In order to achieve high luminosity, PEP-II is designed with two rings to carry the counter-rotating beams. Unlike other circular electron-positron colliders, which have a common closed orbit for both beams, PEP-II depends on mechanical alignment to bring two beams together at the interaction point. This introduces the problem of beams colliding with an offset. Simulations were performed to investigate this.

Figure 6 gives the PEP-II LER tail distribution for various misalignments. Again, the parameters are from the PEP-II CDR. The beam sizes at the IP is 6 μm in vertical and 155 μm in horizontal. In figure 6(a) there is no offset at the collision point. In figure 6(b) and (c), the vertical offset is 2 μm and 6 μm respectively, and the horizontal offset is zero. In 6(d) through 6(f), the vertical offset is zero but horizontal offsets were set to 30, 50, and 150 μm, respectively. From figure 6, one can draw the conclusion that the horizontal offset drives large horizontal tails, while the vertical offset blows up the vertical core. The offsets are not a problem if alignment errors are controlled to a fraction of the beam sizes.

The essential physics behind this result is a breaking of the symmetry of the beam-beam force, that allows odd order resonances to be excited. Therefore, the conclusion from this particular case is not general, since it depends on near-by resonances.

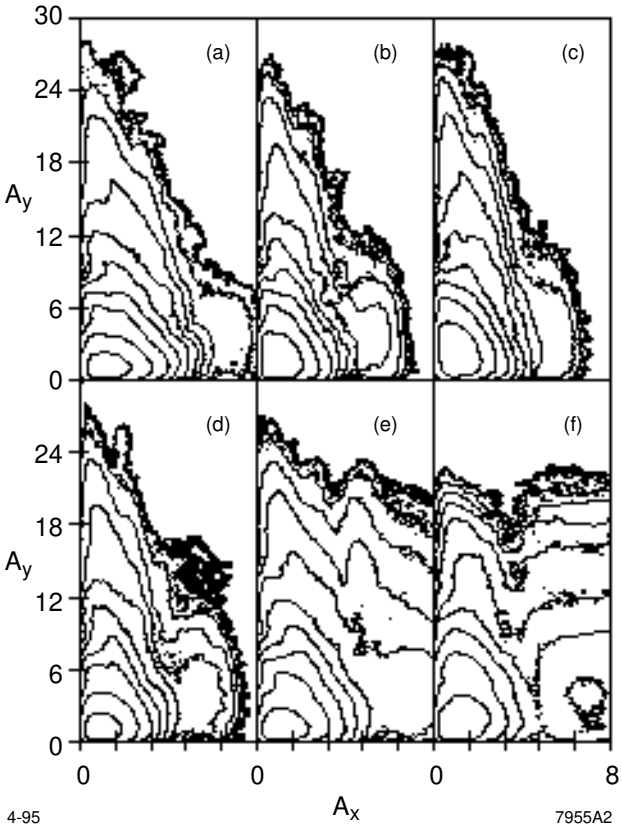

Figure 6. Beam-beam tail distribution of PEP-II LER with offset at the IP. (a): x_{off}=0,y_{off}=0; (b): x_{off}=0,y_{off}=2 μm; (c): x_{off}=0,y_{off}=6 μm; (d): x_{off}=30 μm,y_{off}=0; (e): x_{off}=50 μm,y_{off}=0; (f): x_{off}=150 μm,y_{off}=0.

VI. REFERENCES

[1] J. Irwin, Proc. of the 3rd Advanced ICFA Beam Dynamics Workshop, Novosibirsk, USSR, 123 (1989) /SLAC-PUB-5743,Feb. 1992.

[2] T. Chen, J. Irwin and R. Siemann, Physical Review E, Vol. 49, No. 3, p2323, March 1994.

[3] PEP-II Conceptual Design Report, LBL-PUB-5379 /SLAC-418/CALT-68-1869/UCRL-ID-114055/UC-IIRPA-93-01, (1993).

[4] J. Tennyson, Physica **5D**, 123 (1982).

[5] A.L. Gerasimov and N. Dikansky, Nucl. Instr. Meth. **A292**, 209 (1990); A.L. Gerasimov and N. Dikansky, Nucl. Instr. Meth. **A292**, 221 (1990); A.L. Gerasimov and N. Dikansky, Nucl. Instr. Meth. **A292**, 233 (1990).